Nature of the liquid crystalline phase transitions in the cesium pentadecafluorooctanoate–water system: The nematic–to–smectic-*A* transition

K. W. Jolley
Institute of Fundamental Sciences, Massey University, Palmerston North, New Zealand

N. Boden and D. Parker
Centre for Self-Organising Molecular Systems and School of Chemistry, University of Leeds, Leeds LS2 9JT, United Kingdom

J. R. Henderson
Centre for Self-Organising Molecular Systems and Department of Physics and Astronomy, University of Leeds, LS2 9JT, United Kingdom

(Received 20 November 2001; published 10 April 2002)

Measurements of the diamagnetic susceptibility χ_a, the rotational viscosity coefficient γ_1, and the micellar orientational order parameter S have been made as a function of temperature across the entire nematic phases of cesium pentadecafluorooctanoate (CsPFO)–D_2O samples over the concentration range weight fraction CsPFO w from 0.350 to 0.500. This has been chosen so as to embrace the pseudo-nematic phase–lamellar tricritical point that has been purported to occur at $w=0.43$ (volume fraction $\phi=0.26$). The values of γ_1 vary from about 0.1 $\mathrm{kg\,m^{-1}\,s^{-1}}$ to 1000 $\mathrm{kg\,m^{-1}\,s^{-1}}$ as the temperature decreases across the nematic phase, covering a much larger range than those reported for thermotropic liquid crystals. Measurements of γ_1 have been made much closer to the critical temperature T_{LN} than have previously been reported [$(T-T_{LN})/T_{LN}=2\times10^{-5}$ for the $w=0.350$ sample]. The rotational viscosity critical exponents x calculated from the divergence of γ_1 on approaching the nematic-phase–to–lamellar transition are found to be constant at 2/3 independent of the concentration. These values differ from those of 1/3 and 1/2, respectively, predicted by the He-like three-dimensional XY and mean-field models, in combination with mean-field dynamical relaxation. However, the former would be supported if complete Fisher renormalization (at $\alpha=1/2$) was appropriate over an extended concentration range. Alternatively, this could be an indication of the importance of coupling between the micellar rotational dynamics and critical fluctuations since the latter are seen to be predominant across the entire temperature range of the nematic phase as revealed in the temperature dependence of γ_1.

DOI: 10.1103/PhysRevE.65.041713 PACS number(s): 64.70.Md

I. INTRODUCTION

Salts of short chain perfluorocarboxylic acids form aqueous solutions of disklike micelles that are exceptionally stable over wide concentration intervals. With increasing concentration the disklike micelles undergo a sequence of ordering transitions to form, first, a nematic N_D phase and, subsequently, a smectic lamellar phase [1–8]. These transitions have been attributed to predominantly hard particle interactions between the micelles [6]; that is, the isotropic-to-nematic transition occurs when the surfactant volume fraction ϕ attains a critical proportion of the axial ratio $e=a/b$ of the micelles, where a is the length of the minor, or symmetry axis, and b the length of the major, or perpendicular axis. The form of the temperature–versus–volume-fraction phase diagram is therefore determined by the factors that govern the variations of the size of the micelle with temperature and concentration. As this is qualitatively similar for the entire class of surfactants, a generic phase behavior obtains. The archetypal surfactant is cesium pentadecafluorooctanoate (CsPFO). A partial phase diagram for the CsPFO-D_2O system was published in 1979 [1], and a more detailed and complete version, reproduced in Fig. 1, in 1987 [3]. The phase diagram in H_2O is very similar but with the transition temperatures a few degrees lower [5].

In the CsPFO-D_2O system the N_D^+ phase (the + sign denotes that the mesophase is diamagnetically positive) is stable for weight fractions w between 0.225 (volume fraction $\phi=0.121$) and 0.632 ($\phi=0.449$) and temperatures T between 285.3 and 351.2 K. It is characterized by long-range correlations in the orientations of the symmetry axes of the micelles. It has been established [9] that the isotropic-to-nematic transition in the CsPFO-water system is first order over the entire range of experimentally accessible concentrations $\phi\sim0.07$–0.35 (the lower limit was achieved through supercooling) and that there is no evidence to support the conjecture that a Landau point is being approached on dilution [10,11]. Nevertheless, the transition appears to be extraordinarily weak: $(T_{IN}-T^*)/T_{IN}\sim10^{-5}$ for $\phi<0.20$ compared to $\sim10^{-3}$ in thermotropic systems [12–15], where T^* is the extrapolated spinodal limit of the isotropic phase and T_{IN} is the temperature at which the nematic phase first appears on cooling, and $(T^+-T_{NI})/T_{NI}\sim10^{-4}$–$10^{-3}$, where T^+ is the extrapolated spinodal limit of the nematic phase and T_{NI} is the temperature at which isotropic phase first appears on heating [16]. The density gap $(\phi_{NI}-\phi_{IN})/\phi_{IN}\sim0.33\%$ for $\phi<0.20$ is remarkably small. Furthermore, on the nematic side, the order parameter exponent $\beta=0.34(2)$ differs from either the classical value 0.5 [17–19] or the tricritical value 0.25 [20], both of which have been claimed to apply to thermotropic systems (the tricritical value has also been obtained from Monte Carlo thin hard disk simula-

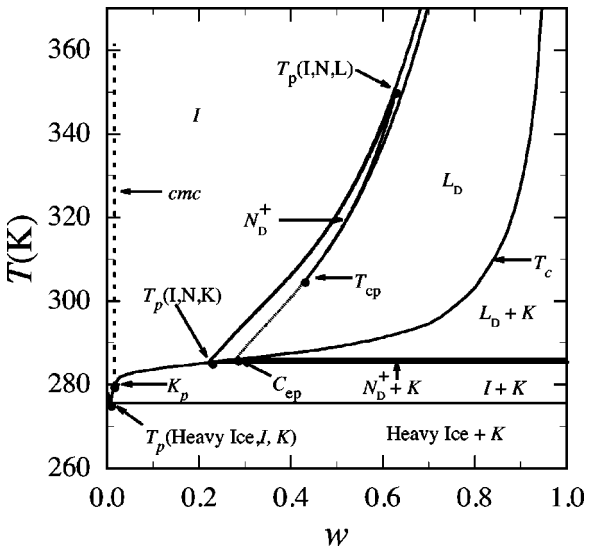

FIG. 1. Phase diagram for the CsPFO-D_2O system. Nomenclature: *I*, isotropic micellar solution phase (to the right of the cmc line); N_D^+, discotic nematic phase with positive diamagnetic susceptibility; L_D, discotic lamellar phase; *K*, CsPFO crystal; T_{cp}, the lamellar-nematic tricritical point; T_p(Heavy Ice,*I*,*K*), the heavy ice–isotropic solution–crystal triple point; $T_p(I,N,K)$, the isotropic micellar–nematic–crystal triple point; $T_p(I,N,L)$, the isotropic micellar solution–nematic–lamellar triple point; C_{ep}, the critical end point; K_p, the Krafft point; T_c, the solubility curve.

tions [21]). Only the entropy change per micelle (*vis-à-vis* molecule for thermotropics) at the transition is comparible for the two kinds of systems. It has been suggested [9] that the anomalously narrow spinodals and value of β might stem from the fundamental differences in the fluctuations in micellar systems compared to typical thermotropic systems. In particular, the internal micellar structure represents a new degree of freedom (self-assembly) that can couple to order parameter and density fluctuations [22]. However, it is recognized that due to the importance of high-order virial coefficients to the Onsager limit of hard disks (in contrast to rods), there is still insufficient theoretical and simulation knowledge to unequivocally rule out substantial agreement with hard-particle models.

The focus in this paper is the nematic-to-smectic transition. This transition is perceived to solely involve the positional ordering of disklike micelles into planes arranged periodically along the nematic director ***n***, and, as such, the smectic phase can be referred to as a discotic lamellar phase L_D. The N_D^+-to-L_D transition is characterized by an apparent tricritical point $T_{cp}(w=0.43;\phi=0.26;T=304.8\ \mathrm{K})$ at which the transition appears to change from continuous to first order (see Fig. 1). Such behavior can be linked to the persistence of disklike micelles together with order-disorder transitions similar to those in thermotropic liquid crystals. The origin of this pseudotricritical point has been qualitatively explained [23] by a modification of the McMillan model [24,25] for the nematic–to–smectic-*A* transition in thermotropics, with a dominant repulsive force between micelles taking the place of the mutual attraction of the aromatic cores of the calamitic mesogen molecules as the driving force for the transition (although one should note that this is not supported by the McMillan ratio, which remains at $T_{LN}/T_{IN}\sim 0.98$ over the entire concentration range of the nematic phase). However, beyond mean field, coupling of the smectic amplitude to fluctuations in the orientation of the director leads to a theoretical expectation for the transition to be first order and so the presence of the apparent tricritical point may simply be a result of an inability to detect a very small (<0.025 K)N_D/L_D phase coexistence region [5].

In thermotropic systems the nematic-smectic-*A* transition has been extensively studied and, in spite of the universality predicted by theory, the experimental critical exponents are not universal [26]. Corresponding studies on the nematic to lamellar transition in lyotropic liquid crystals are, however, scarce. In the CsPFO-water system the critical exponent α for the heat capacity has been shown to be close to zero, suggesting three-dimensional (3D) *XY*-type behavior [10]. In a recent synchrotron x-ray study [27], however, the critical exponent for the longitudinal correlation length $\nu_\parallel$ was determined to be 0.86, a value at odds with the 3D-*XY* model value. Critical exponents have also been obtained for the divergence of the twist viscosity γ_1/χ_a, where γ_1 is the rotational viscosity and χ_a is the anisotropy in the diamagnetic susceptibility. This quantity diverges strongly at T_{LN} with a critical exponent *x*, the value of which is determined by the critical exponents governing the divergence of the relaxation time for the lamellar clusters τ and the longitudinal correlation length $\xi_\parallel$ of the clusters. The Freedericksz effect [28] was used to determine the value of *x* in the CsPFO-water system over the concentration range $w=0.471$ to $w=0.534$ [29]. At $w=0.471$ and $w=0.500$ a value of 0.5 was reported, which increased with increasing CsPFO concentration to 0.69 at $w=0.518$ and to 0.85 at $w=0.534$. In a study of the reorientation times of the nematic director in a magnetic field [30], values for *x* of 0.71, 0.76, 0.77, and 0.85 were obtained for CsPFO-D_2O samples with $w=0.41$, 0.48, 0.50, and 0.55, respectively. In an earlier study on the ammonium heptadecafluorononanoate–H_2O system [31], the same authors reported *x* values of 0.71 and 0.68 for $w=0.232$ and 0.302 samples, respectively.

It is not clear why the exponents reported generally increase with increasing concentration of surfactant. In the Wong study [29], it was postulated that the reason for this increase from the mean-field value of $x=0.5$ was due to Fisher renormalization as a tricritical point was approached at $w=0.60$. The location of the pseudotricritical point has, however, subsequently been shown to be at $w<0.43$ [5] in the CsPFO-D_2O system.

Here we report on careful measurements of γ_1 in the CsPFO-D_2O system on samples with concentrations *w* from 0.350 to 0.500 that encompass the concentration of the pseudotricritical point. Measurements are made much closer to the critical temperatures T_{LN} than previously, with $T-T_{LN}/T_{LN}$ as low as 2×10^{-5} for the $w=0.350$ sample. In addition, nuclear magnetic resonance (NMR) spectroscopy [3,5,32,33] is employed to precisely locate the phase transition temperatures for the actual samples used in the rotational viscosity measurements. It will be shown that the

value for the rotational viscosity critical exponent has a constant value of 2/3 along the N_D-to-L_D transition line, which compares with the corresponding value of 1/3 reported for thermotropic liquid crystals [34]. This doubling of the critical exponent is suggestive of Fisher renormalization, but only if the influence of the pseudotricritical point (i.e., $\alpha = 0.5$) extends throughout the entire experimental concentration range. An alternative reason for the discrepancy is raised.

II. MATERIALS AND METHODS

A. Sample preparation

CsPFO was prepared by neutralizing aqueous solutions of pentadecafluorooctanoic acid (Aldrich Chemical Company Inc.) with cesium carbonate (BDH, Ltd.). The neutralized solution was freeze dried and the salt recrystallized twice from 50% v/v *n*-butanol/*n*-hexane. Residual solvent was removed by heating the salts to 30 °C under vacuum (5×10^{-4} bar) for at least 48 h. Deuterium oxide (Aldrich 99.6 at. %D) was used without further purification.

Conductivity and NMR samples were prepared by weighing CsPFO and D_2O into glass vials, to a precision of 0.02 mg, using a Mettler AT 261 Delta Range balance. The vials were then flame sealed and the samples thoroughly mixed in the isotropic phase before being transferred into conductivity cells or NMR tubes accordingly.

B. NMR measurements

^{2}H NMR spectra were measured with a JEOL GX270 spectrometer operating at 41.34 MHz. ^{2}H spectra were obtained using 16 K data points over a frequency range of 1.0 kHz at a frequency resolution of 0.125 Hz per data point. Four accumulations at a repetition rate of 2 s were used for all spectra. Sample temperatures were regulated using a computer controlled double-pass water-flow sample thermostat [35]. This minimized temperature gradients and enabled the temperature to be controlled to a precision of ± 0.005 K.

C. Electrical conductivity measurements

Electrical conductivity measurements were carried out using an apparatus previously described [36] in which the electric field is generated by a pair of 10 mm $\times$ 10 mm platinized squares placed 10 mm apart. The sample was contained in a double-water-flow cell, which was then located between the poles of a Varian V-3603 electromagnet that could be rotated about the vertical axis. The CsPFO-D_2O system is diamagnetically positive and in the presence of a magnetic field the nematic director $\boldsymbol{n}$ undergoes spontaneous alignment along the field direction. By rotation of the magnet, the angle between the nematic director and the applied electric field $\boldsymbol{E}$ can be systematically varied.

D. Magnetic susceptibility measurements

Magnetic susceptibilities were determined using a Quantum Design superconducting quantum interference device magnetometer operating at a magnetic flux density of 5 T. Both the CsPFO and the heavy water were treated to remove oxygen prior to sample preparation, the former by storing samples under vacuum for four days and the latter by saturating with dry, oxygen free nitrogen. CsPFO-D_2O samples were stored in teflon capped sample tubes under a nitrogen atmosphere. Immediately prior to measurement, about 0.1 g of sample was placed in a 5 mm o.d. quartz electron spin resonance tube and sealed under a stream of helium. Measurements were made on heating from the lamellar into the isotropic phase in 0.5 K increments through the single phase regions and 0.2 K increments close to the phase transition temperatures. At each temperature 50 readings were taken and the mean and standard deviation from the mean displayed.

III. EXPERIMENTAL RESULTS

A. Order parameter measurements

Micellar orientational order parameters for the three samples were calculated from electrical conductivity and small-angle-x-ray scattering (SAXS) measurements [37,38] using a procedure already described [4,39,40]. It rests on the assumption that for nonconducting, ellipsoidal micelles undergoing orientational fluctuations with respect to the director of a uniaxial mesophase the electrical conductivity transforms as a second rank tensor with a principal axes system coincident with that of the moment of inertia tensor [39–42]. That is, the experiment measures the partially averaged component $\tilde{\kappa}_{zz}$ of the conductivity tensor along the direction of $\boldsymbol{E}$, which is taken to be along the z axis of the laboratory frame $L(x,y,z)$. This is given by

$$\tilde{\kappa}_{zz}(\phi) = \kappa_i + \frac{2}{3} P_2(\cos\phi) S(\kappa_\parallel - \kappa_\perp)_M , \qquad (1)$$

where ϕ is the angle between $\boldsymbol{n}$ and $\boldsymbol{E}$, and κ_i is the trace of the conductivity tensor $\boldsymbol{\kappa}$ as measured in the isotropic phase ($S=0$) and in the liquid crystalline phases when $\phi = 54°\ 44'$ [i.e., $P_2(\cos\phi)=0$]. $(\kappa_\parallel)_M$ and $(\kappa_\perp)_M$ are the conductivities measured parallel and perpendicular to the micellar symmetry axis in the frame $M(a,b,c)$ and may be interpreted as $\tilde{\kappa}_{zz}(0°)$ and $\tilde{\kappa}_{zz}(90°)$ in a perfectly ordered system ($S=1$). The electrical conductivities $\tilde{\kappa}_{zz}(\phi)$ and the conductivity anisotropies $\Delta\tilde{\kappa}/\kappa_i [\Delta\tilde{\kappa} = \tilde{\kappa}_{zz}(90°) - \tilde{\kappa}_{zz}(0°)]$ measured as a function of temperature in the three experimental samples are summarized in Fig. 2. The anisotropies in the conductivity at T_{LN} for the $w=0.425$, and 0.500 samples are, respectively, 0.28 and 0.27 and compare with the corresponding values 0.30, and 0.32 from the anisotropies $\Delta\tilde{D}/D_i$ in the heavy-water self-diffusion coefficients as measured by the pulse field gradient NMR experiment [43]. We note that the reasonable agreement between these two sets of data confirm that the conductivity anisotropies measured here and previously reported are essentially correct, despite comments to the contrary [30]. We can now proceed, therefore, to confidently use the conductivity measurements to calculate the micellar orientational order parameter S. To achieve this, we have rearranged Eq. (1) to obtain

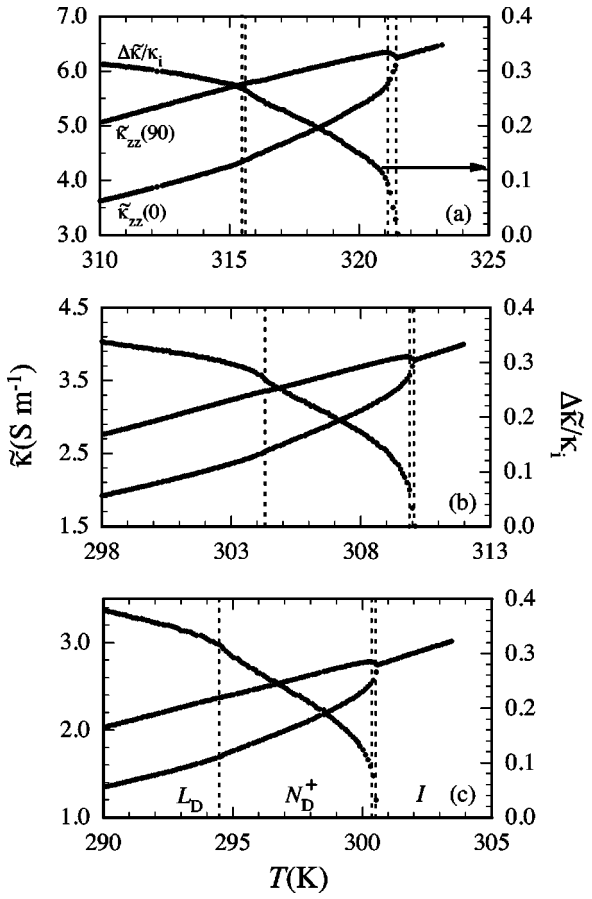

FIG. 2. The electrical conductivity $\tilde{\kappa}_{zz}(\phi)$ and conductivity anisotropy $\Delta\tilde{\kappa}/\kappa_i$ as a function of temperature in samples of CsPFO-^2H_2O with $w=0.500$ (a), 0.425 (b), and 0.350 (c). The phase transition boundaries represented by the vertical dotted lines were determined from NMR measurements [3,5,32] on samples identical to the ones used in the conductivity measurements.

$$\frac{\Delta\tilde{\kappa}}{\kappa_i}=S\frac{(\kappa_\parallel-\kappa_\perp)_M}{(2\kappa_\perp/3+\kappa_\parallel/3)_M}. \tag{2}$$

Values for $\kappa_\parallel$ and $\kappa_\perp$ in the micellar reference frame were calculated [39] from the axial ratios of the micelles (Fig. 3). Substitution of the results into Eq. (2) gave the values for S summarized in Fig. 4. Our values of S for the $w=0.425$ sample at T_{LN} and T_{NI} are 0.74 and 0.23, respectively, which compare favorably with the values of 0.7 and 0.2 obtained from heavy-water self-diffusion measurements on a $w=0.40$ sample [43]. This latter study also reports a decrease in the value of S at both T_{LN} and T_{NI} with increasing concentration. Our results are in agreement with the former observation but show the expected reduction of S at T_{NI} as the nematic-to-isotropic transition weakens with decreasing volume fraction of CsPFO [9].

We note that on approaching the nematic-to-lamellar transition from above, the order parameter appears to diverge. However, we have found that this is far too weak to be able to extract reliable values for the order parameter critical exponent.

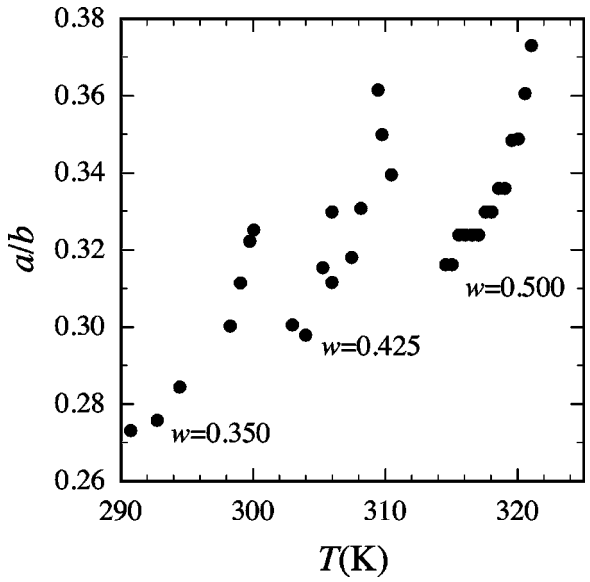

FIG. 3. Axial ratios a/b of the micelles, as obtained from SAXS data for CsPFO-D_2O [37,38]. The data were obtained from the micelle volumes assuming the micelle to be an oblate ellipsoid with minor axis length a of 2.2 nm.

B. Magnetic susceptibility measurements

For a macroscopically aligned nematic or lamellar phase the magnetometer provides a measure of the mass susceptibility $\chi_\parallel^g$ parallel to the nematic director, which is spontaneously aligned parallel to the applied magnetic field direction for a N_D^+ phase, whilst in the isotropic phase the measured quantity is $\chi_i^g=3\chi_\perp^g/2+\chi_\parallel^g/2$, where $\chi_\perp^g$ is the mass susceptibility perpendicular to the nematic director. Since the mass susceptibility is temperature independent, the anisotropy in the mass susceptibility χ_a^g can be calculated from [44]

$$\chi_a^g=\chi_\parallel^g-\chi_\perp^g=\frac{3}{2}(\chi_\parallel^g-\chi_i^g). \tag{3}$$

The temperature dependence of χ_a^g for the CsPFO-D_2O ($w=0.425$) sample is shown in Fig. 5. Also shown on this figure are calculated values for χ_a^g using the model outlined in the Appendix. The close agreement between the calculated and experimental values has led us to adopt the same procedure to calculate the corresponding values for the other two samples. The results are shown in Fig. 6.

C. Rotational viscosity coefficients

The nematic phase of the CsPFO-water system is diamagnetically positive, i.e., the director ***n*** undergoes spontaneous alignment along the direction of an applied magnetic field ***H*** to give a macroscopically aligned uniaxial mesophase. If the direction of ***H*** is suddenly changed the nematic director will experience a magnetic torque, which causes it to rotate back to its equilibrium position along ***n***. The rate of angular rotation of ***n*** is given by [45]

$$\frac{d\phi}{dt}=\frac{\sin\phi\cos\phi}{\tau_D}, \tag{4}$$

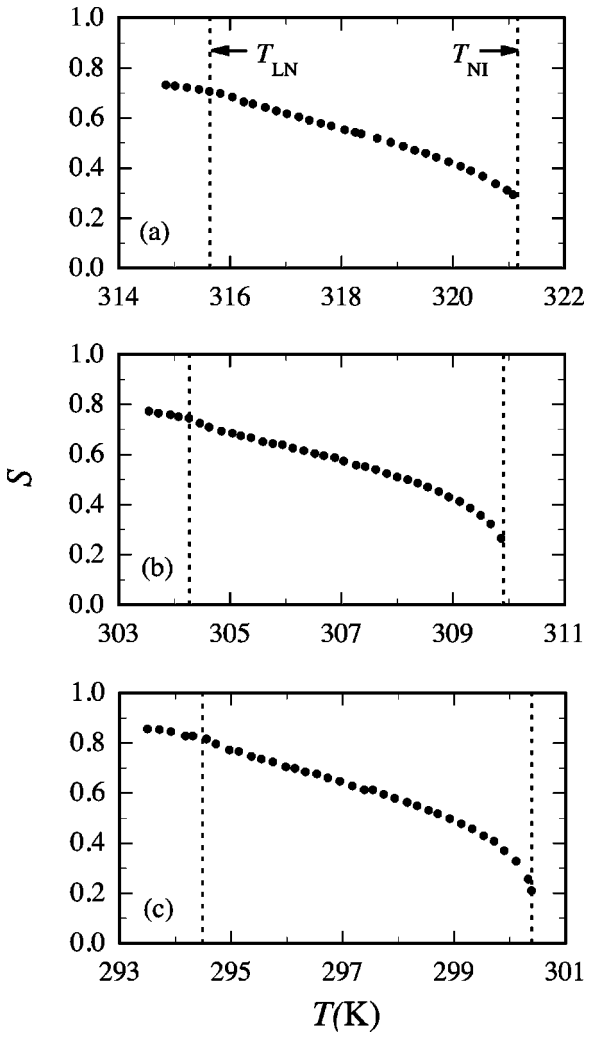

FIG. 4. Orientational order parameters S as a function of temperature across the nematic phases of CsPFO-^2H_2O samples with $w=0.500$ (a), 0.425 (b), and 0.350 (c).

where ϕ is the angle between $\boldsymbol{H}$ and $\boldsymbol{n}$ and τ_D, the director relaxation time, is related to the rotational viscosity γ_1 by

$$\tau_D=\frac{\mu_0\gamma_1}{\chi_a H^2}. \tag{5}$$

Here μ_0 is the permittivity of free space, χ_a $(=\chi_a^g\rho)$ is the diamagnetic susceptibility anisotropy, and H is the magnitude of the magnetic field. Integration of Eq. (4) between the limits of ϕ_0 at time zero and ϕ_t gives

$$\tan\phi_t=\tan\phi_0\exp(-t/\tau_D). \tag{6}$$

The director relaxation time τ_D, and hence the ratio γ_1/χ_a, can thus be obtained from measurement of the time evolution of ϕ_t. This is readily accomplished by the measurement of the electrical conductivity following an initial rotation of the magnetic field away from the director as described below.

The magnet was first rotated so as to establish an angle of 20° between $\boldsymbol{n}$ and $\boldsymbol{E}$ (i.e., $\phi_0=20°$). The magnet was then rapidly rotated (~ 1 s) so as to align $\boldsymbol{E}$ and $\boldsymbol{H}$ and measurement of $\tilde{\kappa}_{zz}(\phi_t)$ initiated. As the director reorientates $\tilde{\kappa}_{zz}(\phi_t)$ decreases to eventually reach a constant equilibrium value $\tilde{\kappa}_{zz}(0°)$. Using Eq. (1), ϕ_t can be expressed in terms of the conductivity at the beginning $\tilde{\kappa}_{zz}(\phi_0)$, during $\tilde{\kappa}_{zz}(\phi_t)$ and at the end (thermal equilibrium) of the experiment $\tilde{\kappa}_{zz}(\phi_\infty)$ $[=\tilde{\kappa}_{zz}(0°)]$, through the equation

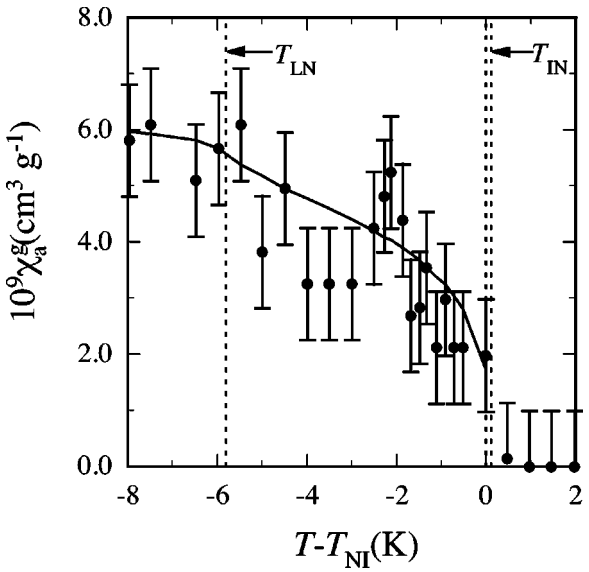

FIG. 5. The temperature dependence of the anisotropy in mass susceptibility for a CsPFO-D_2O($w=0.425$) sample. The solid line has been calculated from a knowledge of the temperature dependence of the orientational order parameter (Fig. 4) and the axial ratio a/b of the micelle (Fig. 3), as outlined in the Appendix.

$$\cos^2\phi_t=1+\frac{[\kappa_{zz}(\phi_t)-\kappa_{zz}(\phi_\infty)][\cos^2\phi_0-1]}{\kappa_{zz}(\phi_0)-\kappa_{zz}(\phi_\infty)}. \tag{7}$$

The angle ϕ_0 was chosen to be 20° since this precludes the possibility of the generation of macroscopic fluid motions in the liquid crystal caused by too great a magnetic torque [46]. In provisional experiments it was established that γ_1/χ_a was independent of the magnitude of the magnetic field used. In practice, H was chosen within the range 0.5 to 2 T so the period over which the relaxation was monitored ($\approx 3\times\tau_D$) was between 3 to 5 min. At temperatures close to T_{LN}, where γ_1/χ_a is rapidly diverging this was not practicable. At these temperatures the maximum field of 2 T was used and the relaxation followed for about 30 min. Experimental values for T_{LN} were determined by first cooling an oriented sample ($\phi=0°$) into the lamellar phase before rotating the field to produce a sample with $\phi=20°$. The conductivity was then monitored as the temperature was increased in 10 mK steps waiting 10 min at each temperature. Director relaxation, and thus the location of T_{LN} to a precision of ± 0.005 K, was indicated by a sudden decrease in the conductivity. The phase transition temperatures determined in this manner were identical, within experimental error (0.005 K), to those determined through NMR measurements on identical samples.

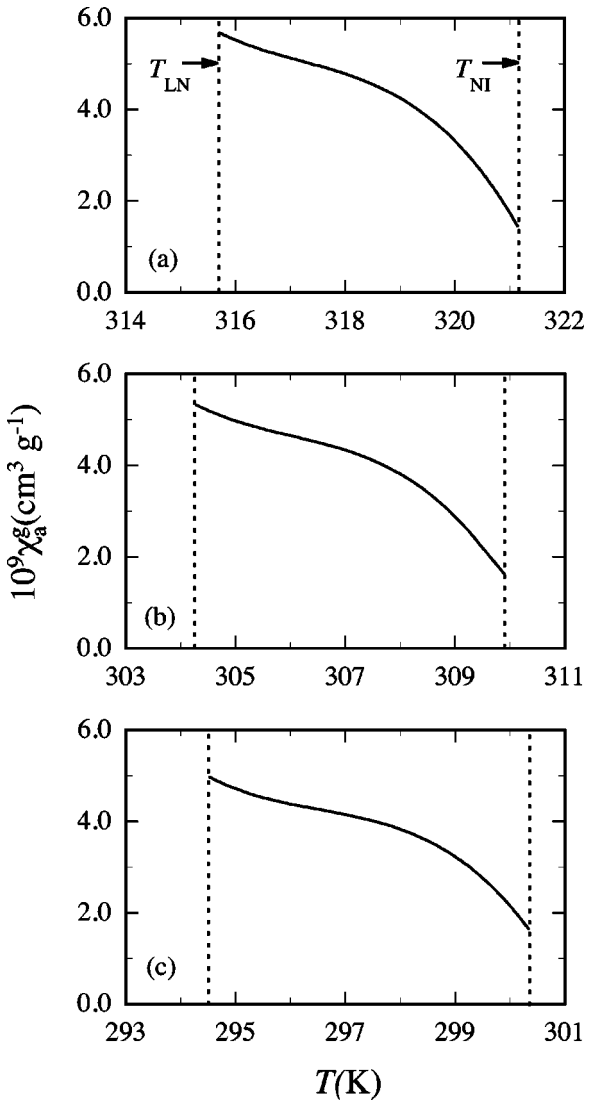

FIG. 6. The anisotropy in the mass susceptibility as calculated using the model described in the Appendix for CsPFO-D_2O samples with $w=0.500$ (a), 0.425 (b), and 0.350 (c).

For the $w=0.350$ sample the director relaxation was well described by Eq. (6) at all temperatures. For the $w=0.500$ sample the relaxation became complex for temperatures in the range $T_{LN}<T<(T_{LN}+0.08\ \mathrm{K})$. The nematic-to-lamellar transition is first order for this sample and the complex relaxation behavior is a consequence of two-phase nematic/lamellar coexistence. The $w=0.425$ sample also showed complex relaxation behavior at temperatures within about 15 mK of the measured T_{LN}. This is most probably due to a narrow two-phase coexistence region indicating that the transition is still weakly first order at this concentration. This observation is seemingly in conflict with the estimated T_{cp} value of $w=0.43$ as obtained from NMR measurements [5]. There is, however, good reason to believe that below the apparent T_{cp} the transition is fluctuation-induced first order [47] and director relaxation is a more sensitive indication of a mixed phase region than is NMR. No attempt was made to extract rotational viscosity coefficients from data collected in mixed phase regimes.

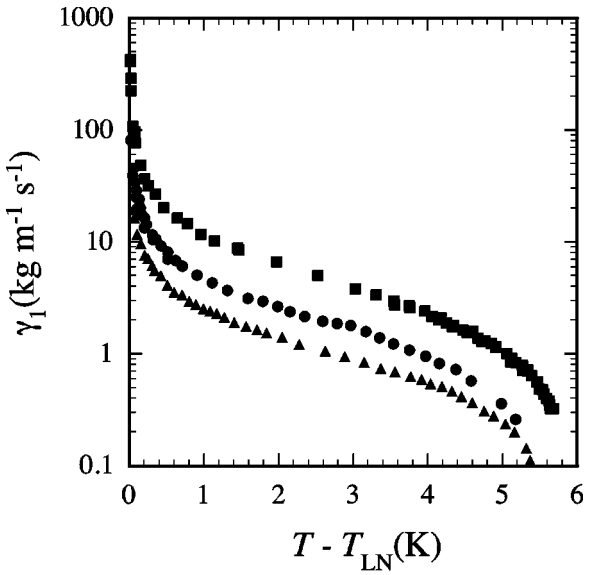

FIG. 7. Temperature dependence of the rotational viscosity γ_1 for CsPFO-D_2O samples with $w=0.350$ (squares), 0.425 (circles), and 0.500 (triangles).

The temperature dependence of the rotational viscosities γ_1 are shown in Fig. 7. These were obtained by multiplying the γ_1/χ_a values by the corresponding anisotropies in volume susceptibilities χ_a, which were calculated as described in the Appendix. The γ_1 values for CsPFO-D_2O are similar in magnitude to those measured (0.1 to 100 $\mathrm{kg\,m^{-1}\,s^{-1}}$ over the discotic nematic temperature range of 22 K [48]) for a decylammonium chloride–NH_4Cl–water sample {DACl:NH_4Cl ratio 10:1; 52 % water}, and to values measured in the tetradecacetylammonium bromide–D_2O [49] and potassium laurate–1-decanol–D_2O [50] systems. Values of γ_1 are much smaller for thermotropic nematic phases; typically from 0.02 to 0.2 $\mathrm{kg\,m^{-1}\,s^{-1}}$, as for example, across the nematic range of *N-p*-methoxybenzylidene-*p*-butylaniline [51].

D. Calculation of critical exponents

Critical exponents for the divergence of γ_1 were obtained in two ways. First by fitting the data in Fig. 7 within 1.5 K of T_{LN}, where critical divergence is clearly apparent, to the equation

$$\gamma_1=A(T/T^*-1)^{-x}. \tag{8}$$

The best-fit lines to these fits are shown in Fig. 8(a) and the corresponding critical exponents and temperatures in Table I. We note that the data shown in Fig. 8 extends to reduced temperatures that are more than an order of magnitude smaller than those previously reported [30] for this system.

The second method involved fitting the data across the entire nematic range to an equation first proposed by Wong [29] to account for the critical component of γ_1,

$$\gamma_1=AS^2\exp(W/T)(T/T^*-1)^{-x}, \tag{9}$$

where W is a measure of the potential barrier due to the local field created by all other molecules in the fluid against which

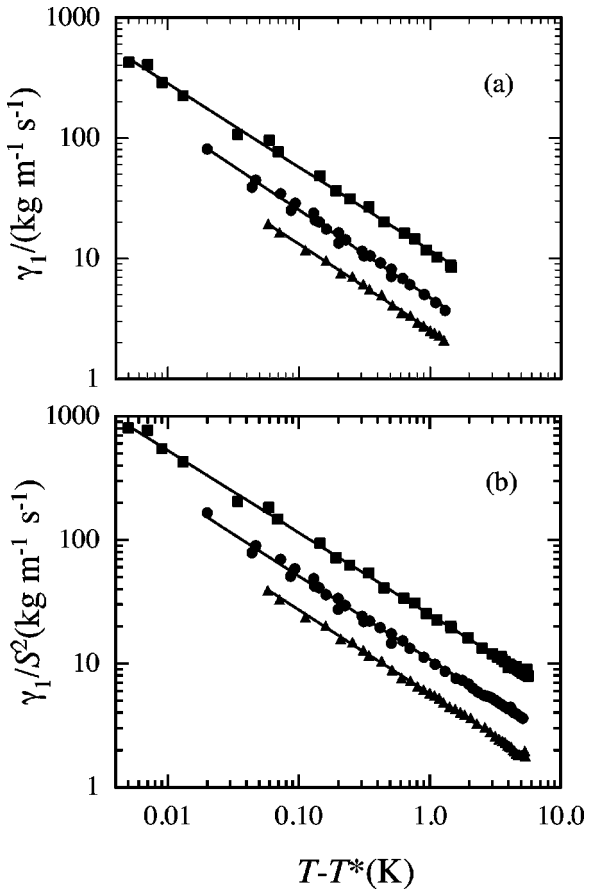

FIG. 8. Plots of (a) γ_1 vs $T-T^*$ within 1.5 K of T^* and (b) γ_1/S^2 vs $T-T^*$ over the entire nematic range, for CsPFO-D_2O samples with $w=0.350$ (squares), 0.425 (circles), and 0.500 (triangles). Best-fit parameters obtained from fitting the data in (a) to Eq. (8) and the data in (b) to Eq. (9) (with $W=0$) are given in Table I.

the director rotates. Setting $W=0$ gave an excellent fit to the data, as shown in Fig. 8(b), and gave critical exponents equal to those obtained by the more restricted fit to Eq. (8) within the errors of the fit. Using nonzero values of W had little effect on the values of x that were obtained. Setting an upper limit on W of 5000 K [29], for example, resulted in decreases of only 0.03 in the best-fit critical exponents [38].

IV. DISCUSSION

A. Critical exponents

The concentration independent value for the twist viscosity critical exponent x obtained in this study is in conflict with the results of other workers [29–31] who generally found an increase in x with increasing surfactant concentration. A likely reason for this is that, due to an uncertainty in the location of T_{NL}, measurements on the high w samples were made in the N_D-L phase coexistence regime. In the present study, NMR measurement located T_{NL} to within 5 mK and γ_1 measurements were always made in homogeneous N_D phases. Moreover, a knowledge of the precise phase transition temperatures enabled measurements to be made much closer to the critical temperatures than those previously reported.

TABLE I. T_{LN} values as measured by NMR and best-fit parameters to Eqs. (8) and (9) (see text).

w	T_{LN} (K)	T^* (K)	x
0.350	294.47(1)	294.47(1)	0.66(3)
0.425	304.28(1)	304.27(1)	0.69(3)
0.500	315.65(1)	315.64(1)	0.67(3)

The CsPFO-D_2O system is unusual in that critical behavior associated with the presence of lamellar domains is present throughout the entire nematic range and is particularly dominant close to T_{LN}. The excess viscosity $\delta\gamma_1$ associated with these lamellar domains is proportional to τ/ξ, where τ is the relaxation time for the lamellar clusters and ξ the coherence length of these clusters [52]. The temperature dependence of γ_1 depends on both τ and ξ. Using the mean-field approximation, McMillan [53] predicted the critical exponent for the divergence of the viscosity to have the value 0.5, i.e., the critical exponents for τ and ξ are 1 and 0.5, respectively. The three-dimensional XY model, on the other hand, has a critical exponent for the divergence of ξ of 0.66, and thus predicts a critical exponent of 0.33 for the divergence of the viscosity assuming that τ remains a mean-field quantity [54]. Thus, neither model is able to account for our observation of a constant critical exponent of $x=2/3$ along the nematic to lamellar transition line.

The measured values for ν, the critical exponent for the divergence of ξ are often different from the predictions of both the mean-field and 3D-XY models [26]. Indeed, a recent x-ray synchrotron x-ray scattering study of a CsPFO-H_2O solution ($w=0.466$) [27] showed that $\xi_\parallel$ exhibits a single power law divergence with a critical exponent $\nu_\parallel$ of 0.86(4), behavior typical of thermotropic liquid crystals with $T_{NA}/T_{NI}\sim 0.92$. Using this value for $\nu_\parallel$ would suggest a viscosity critical exponent x of 0.14.

The most obvious theoretical explanation for the problems in obtaining consistent values for a variety of exponents is Fisher renormalization on approach to a tricritical point [29,55]. The extent of influence of a nearby tricritical point, the crossover region, is nonuniversal and varies with the fourth power of the transition temperature gradient in the T,w plane [55]. From Fig. 1, this gradient is relatively high for the CsPFO-D_2O system, implying a strong influence from the pseudotricritical point. Nevertheless, there is little suggestion in our data of any variation of the exponent x with CsPFO concentration. From Table I this explanation would require almost complete doubling (appropriate to $\alpha=1/2$) of the exponent over a wide concentration range. The underlying exponent would then be that appropriate to the 3D-XY model, but the lack of the merest hint of a concentration dependence seems problematical. We therefore raise a second possibility that the mean-field exponent of 1.0 for τ may not be appropriate for micellar nematic systems. This exponent depends on the mesophase dynamics for rotation of the nematic director that may be strongly influenced by fluctuations. These prevail across the entire nematic phase in the

CsPFO-D_2O system whilst in thermotropic systems there is a strong contribution from noncritical viscosity behavior. In a previous paper on the isotropic-to-nematic transition in the CsPFO-D_2O system [9] we argued that the anomalously narrow spinodals and nonclassical value of the order parameter on the nematic side may stem from fundamental differences in the fluctuations in micellar systems compared to the typical thermotropic systems. Similarly, fluctuations may be responsible for the exceptionally narrow smectic lamellar–nematic biphasic region for our system, for which the mean-field McMillan parameter wrongly indicates a strong first order transition (see below).

B. Phase behavior

The topology of the phase diagrams of fluorosurfactant systems is characteristically different from the form of that associated with hydrocarbon surfactant–water mixtures. In these latter systems, the phase transitions are driven by changes in the stability of the various aggregate structures with increasing surfactant concentration. This gives rise to phase diagrams in which the associated phase areas are arranged sequentially across the phase diagram with upper boundaries terminated by a singular point. In contrast, in the CsPFO-water system the nematic phase is sandwiched between the isotropic and smectic lamellar phases and extends, in the CsPFO-D_2O system, from $\phi=0.121$, $T=285.3$ K to $\phi=0.449$,$T=351.2$ K. It is this behavior that gives rise to the L-to-N_D-to-I sequence of phase transitions on raising the temperature, behavior that is predicted by the McMillan model [24,25]. However, in the CsPFO-D_2O system the McMillan ratio T_{NL}/T_{IN} varies from 0.98 at $\phi=0.150$ to 1.0 at $\phi=0.426$, which is anomolous for nonaggregate particle systems in the absence of a strong first order transition.

It is interesting to note that a recent x-ray study [27] on the CsPFO-H_2O system yielded values for the smectic susceptibility and longitudinal correlation length critical exponents for a $w=0.466$ sample that equates with those expected for a thermotropic liquid crystal system with $T_{NA}/T_{NI}=0.92$, which corresponds to a nematic temperature range of about 25 K at room temperature compared with the observed range of about 5 K. For a $w=0.466$ sample, however, the values of the orientational order parameter at T_{NI} and T_{NL} are ~ 0.3 and ~ 0.8, respectively (Fig. 4), in line with predictions of mean-field theory for second order transitions [56]. The implication of this is that the nematic order parameter increases much faster on lowering the temperature than is the case in thermotropic systems. This behavior might be understood in terms of a coupling between the intramicellar self-assembly degrees of freedom and the nematic order parameter. From the Maier-Saupe [57] relationship $kT_{NI}=0.2202\epsilon$, with $\epsilon=\epsilon_{mm}\phi/V_m$, where ϵ_{mm} ($\epsilon_{mm}\propto\tilde{n}^2$ [58]; $\tilde{n}$ is the average aggregation number of the micelles) is the strength of the anisotropic dispersive interaction between two micelles of volume $V_m(V_m\propto\tilde{n})$, we see that at a particular volume fraction T_{NI} is proportional to $\tilde{n}$. Thus, as $\tilde{n}$ grows and the order parameter increases as the temperature is lowered [4,38], the transition temperature T_{NI} is shifted up, compressing the range of the nematic phase. In other words, the narrow nematic phase is a measure of the coupling between the self-assembly and the nematic order parameter.

C. Structural changes at the smectic-to-nematic transition

Finally, we comment on the yet unresolved issue of the nature of any structural changes of the surfactant aggregates occurring at this transition. Two alternative models have been proposed. In one, the micelles are considered simply to condense onto equidistant planes, driven by free volume entropy considerations as if the micelles were hard particles. Of course, at higher concentrations more complex lamellar structures must ensue in response to micelle packing constraints and interlayer repulsive forces. The alternative proposal is that the transition is driven by a discrete change in aggregate structure from disklike micelles to infinitely extending perforated bilayers. The former is apparently supported by the absence of any discernible changes at the transition in the x-ray scattering pattern [4,40], and the lack of any discontinuities in the micellar order parameter derived from NMR quadrupole splittings [3–5] or from anisotropies in ionic or water diffusion coefficients (obtained, respectively, by electrical conductivity [40,41] and NMR measurements [43]). However, it has been argued that the x-ray diffraction measurements can be interpreted in terms of a model in which perforated bilayers gradually break up as the temperature is raised through the lamellar phase and into and across the nematic phase [59]. The latter is appealing within the context of a dislocation unbinding transition. However, this model would require that disklike micelles are unstable relative to fluid bilayers, which may not necessarily be the case for perfluorocarbon surfactants.

V. CONCLUSIONS

The values of the rotational viscosity critical exponent x have been shown to be 0.66(3) over the concentration range $w=0.350$ to $w=0.500$ ($\phi=0.203$ to $\phi=0.322$). These values differ from those of 1/3 and 1/2, respectively, predicted by the He-like 3D-XY model and mean-field models, in combination with mean-field dynamical relaxation. However, the former would be supported if complete Fisher renormalization (at $\alpha=1/2$) was appropriate over an extended concentration range. Alternatively, this could be an indication of the importance of coupling between the micellar rotational dynamics and critical fluctuations since the latter are seen to be predominant across the entire temperature range of the nematic phase.

The McMillan parameter T_{NL}/T_{NI}, which varies from 0.98 at $\phi=0.150$ to 1.0 at $\phi=0.426$ is exceptionally large for such a weak first order transition. This has been explained as arising from a compression of the nematic phase due to coupling between the micellar self-assembly and the nematic order parameter.

ACKNOWLEDGMENT

We acknowledge the Engineering and Physical Sciences Research Council for support to K.W.J. during his stay at Leeds where this work was done.

APPENDIX

The mass susceptibility anisotropy χ_a^g of a micellar solution is given by

$$\chi_a^g = \chi_{a,\mathrm{mic}}^g NS = \chi_{a,\mathrm{mic}}^g \frac{wN_A}{Mn} S, \tag{A1}$$

where S is the orientational order parameter, N is the number of micelles in the sample, w is the mass of surfactant in the sample, M is the molar mass of CsPFO and n the micelle aggregation number.

The micelle anisotropy is given by

$$\chi_{a,\mathrm{mic}}^g = n\langle P_2(\cos\alpha)\rangle_s \chi_{a,\mathrm{mol}}^g, \tag{A2}$$

where $\chi_{a,\mathrm{mol}}^g$ is the molecular susceptibility and $\langle P_2(\cos\alpha)\rangle_s$, where α is the angle between the normal to the surface and the symmetry axis of the micelle, and the angular brackets denote an average over the surface, is a shape factor that accounts for the spatial distribution of molecules within the micelle. For an oblate ellipsoid, this quantity can be calculated from the axial ratio a/b of the micelle [3]. Combining Eqs. (A1) and (A2) we obtain,

$$\chi_a^g = \frac{wN_A S\langle P_2(\cos\alpha)\rangle}{M} \chi_{a_{\mathrm{mol}}}^g. \tag{A3}$$

From the value of χ_a^g for the $w=0.425$ sample at T_{LN} (Fig. 4) and corresponding values of S (Fig. 4) and $\langle P_2(\cos\alpha)\rangle_s$ (calculated from the a/b ratio at T_{LN} Fig. 3) a value for $\chi_{a,\mathrm{mol}}^g$ of 2.4×10^{-29} $\mathrm{cm^3\,g^{-1}}$ is obtained. Knowing the temperature dependence of S and $\langle P_2(\cos\alpha)\rangle_s$, the temperature dependence of χ_a^g can thus be calculated for all three samples. The mass susceptibility anisotropy is related to the volume susceptibility anisotropy by $\chi_a^g=\chi_a/\rho$, where ρ is the density of the sample. Sample densities are obtained, assuming ideal mixing, from the temperature dependence of the density of D_2O [60] and, in the absence of any temperature dependent data, a density for CsPFO of 2.32 $\mathrm{g\,cm^{-3}}$ [6].

[1] N. Boden, P.H. Jackson, K. McMullen, and M.C. Holmes, Chem. Phys. Lett. **65**, 476 (1979).
[2] N. Boden, K. Radley, and M.C. Holmes, Mol. Phys. **42**, 493 (1981).
[3] N. Boden, S.A. Corne, and K.W. Jolley, J. Phys. Chem. **91**, 4092 (1987).
[4] N. Boden, J. Clements, K.W. Jolley, D. Parker, and M.H. Smith, J. Chem. Phys. **93**, 9096 (1990).
[5] N. Boden, K.W. Jolley, and M.H. Smith, J. Phys. Chem. **97**, 7678 (1993).
[6] N. Boden *et al.*, J. Chem. Phys. **103**, 5712 (1995).
[7] J.P. Dombroski, P.J.B. Edwards, K.W. Jolley, and N. Boden, Liq. Cryst. **18**, 51 (1995).
[8] P.J.B. Edwards, K.W. Jolley, M.H. Smith, S.J. Thomsen, and N. Boden, Langmuir **13**, 2665 (1997).
[9] K.W. Jolley, M.H. Smith, N. Boden, and J.R. Henderson, Phys. Rev. E **63**, 051705 (2001).
[10] S.T. Shin, S. Kumar, D. Finotello, S. Sabol Keast, and M.E. Neubert, Phys. Rev. A **45**, 8683 (1992).
[11] C. Rosenblatt, S. Kumar, and J.D. Litster, Phys. Rev. A **29**, 1010 (1984).
[12] Y.M. Shih, H.M. Huang, and C.W. Woo, Mol. Cryst. Liq. Cryst. **34**, 7 (1976).
[13] C.-P. Fan and M.J. Stephen, Phys. Rev. Lett. **25**, 500 (1970).
[14] T.W. Stinson and J.D. Litster, Phys. Rev. Lett. **25**, 503 (1970).
[15] T.W. Stinson and J.D. Litster, J. Appl. Phys. **41**, 996 (1970).
[16] N. Boden, J. Clements, K.A. Dawson, K.W. Jolley, and D. Parker, Phys. Rev. Lett. **66**, 2883 (1991).
[17] Y. Poggi, J.C. Filippini, and R. Aleonard, Phys. Lett. **57A**, 53 (1976).
[18] Y. Poggi, P. Allen, and J.C. Filippini, Mol. Cryst. Liq. Cryst. **37**, 1 (1976).
[19] Y. Poggi, P. Allen, and R. Aleonarf, Phys. Rev. A **14**, 466 (1976).
[20] J. Thoen and G. Menu, Mol. Cryst. Liq. Cryst. **97**, 163 (1983).
[21] D. Frenkel and R. Eppenga, Phys. Rev. Lett. **49**, 1089 (1982).
[22] P.K. Mukherjee, J. Phys.: Condens. Matter **10**, 9191 (1998).
[23] N. Boden, R.J. Bushby, L. Ferris, C. Hardy, and F. Sixl, Liq. Cryst. **1**, 109 (1986).
[24] W.L. McMillan, Phys. Rev. A **6**, 936 (1972).
[25] W.L. McMillan, Phys. Rev. A **4**, 1238 (1971).
[26] C.W. Garland and G. Nounesis, Phys. Rev. E **49**, 2964 (1994).
[27] S.T. Shin, J.D. Brock, M. Sutton, J.D. Litster, and S. Kumar, Phys. Rev. E **57**, R3711 (1998).
[28] V. Freedericksz, Phys. Z. Sowjetunion **6**, 490 (1934).
[29] M.W.K. Wong, Ph.D. thesis, MIT, 1986.
[30] P. Photinos and A. Saupe, Phys. Rev. A **43**, 2890 (1991).
[31] P.J. Photinos and A. Saupe, J. Phys. Chem. **85**, 7467 (1986).
[32] N. Boden, K.W. Jolley, and M.H. Smith, Liq. Cryst. **6**, 481 (1989).
[33] K.W. Jolley, M.H. Smith, and N. Boden, Chem. Phys. Lett. **162**, 152 (1989).
[34] A.F. Martins, A.C. Diogo, and N.P. Vaz, Ann. Phys. (Paris) **3**, 361 (1978).
[35] N. Boden, S.A. Corne, P. Halford-Maw, D. Fogarty, and K.W. Jolley, J. Magn. Reson. **98**, 92 (1992).
[36] N. Boden, G.R. Hedwig, M.C. Holmes, K.W. Jolley, and D. Parker, Liq. Cryst. **11**, 311 (1992).
[37] M.C. Holmes, D.J. Reynolds, and N. Boden, J. Phys. Chem. **91**, 5257 (1987).
[38] D. Parker, Ph.D. thesis, University of Leeds, 1987.
[39] N. Boden, D. Parker, and K.W. Jolley, Mol. Cryst. Liq. Cryst. **152**, 121 (1987).
[40] N. Boden *et al.*, J. Phys. (Paris) **47**, 2135 (1986).
[41] N. Boden, S.A. Corne, and K.W. Jolley, Chem. Phys. Lett. **105**, 99 (1984).
[42] N. Boden and K.W. Jolley, Phys. Rev. A **45**, 8751 (1992).
[43] H. Johannesson, I. Furo, and B. Halle, Phys. Rev. E **53**, 4904 (1996).

[44] W.H. de Jeu and W.A.P. Claassen, J. Chem. Phys. **68**, 102 (1978).
[45] P.G. De Gennes, *The Physics of Liquid Crystals* (Oxford University Press, New York, 1974).
[46] N. Boden, K. McMullen, and M.C. Holmes, in *Magnetic Resonance in Colloid and Interface Science*, edited by J.P. Fraissard and H.A. Resing (Reidel, Dordrecht, 1980), p. 667.
[47] M.A. Anisimov, V.P. Voronov, A.O. Kulkov, V.N. Petukhov, and F. Kholmusodov, Mol. Cryst. Liq. Cryst. **150b**, 399 (1987).
[48] E. Zhou, M. Stefanov, and A. Saupe, J. Chem. Phys. **88**, 5137 (1988).
[49] P. Photinos, S.Y. Xu, and A. Saupe, Phys. Rev. A **42**, 865 (1990).
[50] P.J. Photinos, G. Melnik, and A. Saupe, J. Chem. Phys. **84**, 6928 (1986).
[51] W.H. de Jeu, *Physical Properties of Liquid Crystalline Materials* (Gordon and Breach, New York, 1980).
[52] S. Chandrasekhar, *Liquid Crystals* (Cambridge University Press, Cambridge, 1992).
[53] W.L. McMillan, Phys. Rev. A **9**, 1720 (1974).
[54] F. Brochard, J. Phys. (Paris) **34**, 411 (1973).
[55] J.P. Hill, B. Keimer, K.W. Evans-Lutterodt, R.J. Birgeneau, and C.W. Garland, Phys. Rev. A **40**, 4625 (1989).
[56] R.L. Humphries, P.G. James, and G.R. Luckhurst, J. Chem. Soc., Faraday Trans. **72**, 996 (1972).
[57] W. Maier and A. Saupe, Z. Naturforsch. A **14A**, 882 (1959).
[58] N. Boden, in *Micelles, Membranes, Microemulsions and Monolayers*, edited by W.M. Gelbart, A. Ben-Shaul, and D. Roux (Springer-Verlag, New York, 1994), p. 153.
[59] M.S. Leaver and M.C. Holmes, J. Phys. II **3**, 105 (1993).
[60] G.S. Kell, J. Chem. Eng. Data Ser. **12**, 66 (1967).